https://doi.org/10.5194/cp-2020-147
Preprint. Discussion started: 21 November 2020

Climate of the Past Discussions

The role of land cover on the climate of glacial Europe

Patricio Velasquez[1,2], Jed O. Kaplan[3], Martina Messmer[1,2,4], Patrick Ludwig[5], and Christoph C. Raible[1,2]

[1]Climate and Environmental Physics, Physics Institute, University of Bern, Bern, Switzerland
[2]Oeschger Center for Climate Change Research, University of Bern, Bern, Switzerland
[3]Department of Earth Sciences, The University of Hong Kong, Hong Kong
[4]School of Earth Sciences, The University of Melbourne, Melbourne, Victoria, Australia
[5]Institute of Meteorology and Climate Research, Karlsruhe Institute of Technology, Karlsruhe, Germany

Correspondence: Patricio Velasquez (patricio.velasquez@climate.unibe.ch)

Abstract. Earth system models show wide disagreement when simulating the climate of the continents at the Last Glacial Maximum (LGM). This disagreement may be related to a variety of factors, including model resolution and an incomplete representation of Earth system processes. To assess the importance of resolution and land-atmosphere feedbacks on the climate of Europe, we performed an iterative, asynchronously coupled land-atmosphere modelling experiment that combined a global climate model, a regional climate model, and a dynamic vegetation model. The regional climate and land cover models were run at high (18 km) resolution over a domain covering the ice-free regions of Europe. Asynchronous coupling between the regional climate model and the vegetation model showed that the land-atmosphere coupling achieves quasi-equilibrium after four iterations. Modelled climate and land cover agree reasonably well with independent reconstructions based on pollen and other paleoenvironmental proxies. To assess the importance of land cover on the LGM climate of Europe, we performed a sensitivity test where we used LGM climate but present day land cover as boundary conditions. These simulations show that the LGM land-atmosphere feedback leads to colder and drier conditions around the Alps and a warmer and drier climate in southeastern Europe. Even in mid-latitude Europe where the land-atmosphere coupling strength is generally weak, and under glacial conditions with a southward displacement of the storm track and increased importance of the Atlantic, regional climate is significantly influenced by land cover.

1 Introduction

The Last Glacial Maximum (LGM, 21 ka; Yokoyama et al., 2000; Clark et al., 2009; Van Meerbeeck et al., 2009) is a period of focus for Earth system modelling because it represents a time when boundary conditions were very different from the present and is therefore a good testbed of models' ability to faithfully reproduce a range of climate states (e.g., Mix et al., 2001; Janská et al., 2017; Cleator et al., 2020). In Europe, the LGM is also an interesting period in human history, because small groups of highly mobile Upper Paleolithic hunter-gatherers persisted in the face of inhospitable climate, while Neanderthals disappeared (Finlayson, 2004; Finlayson et al., 2006; Finlayson, 2008; Burke et al., 2014; Maier et al., 2016; Baena Preysler et al., 2019). However, despite more than three decades of research, the LGM climate of the continents is only poorly understood. Global climate models (GCMs) show little agreement in LGM simulations for Europe (Braconnot et al., 2012; Kageyama et al., 2017;

https://doi.org/10.5194/cp-2020-147
Preprint. Discussion started: 21 November 2020

Climate of the Past Discussions

Ludwig et al., 2019; Kageyama et al., 2020). It has been suggested that a reason for the large uncertainty could be related to spatial resolution in the climate models (Walsh et al., 2008; Jia et al., 2019; Ludwig et al., 2019; Raible et al., 2020). Recent advances in high resolution regional climate modelling led to the application of regional climate models to the glacial climate of Europe (e.g.; Ludwig et al., 2020). Here, we further investigate the importance of land cover for climate during this period.

Paleoclimate reconstructions suggest that the climate of Europe was 10 to 14 °C colder and around 200 mm year^{-1} drier during the LGM compared to present day (Wu et al., 2007; Bartlein et al., 2011). However, uncertainties in the paleoclimate reconstructions are large, the few sites with samples dating to the LGM are not uniformly distributed in space (e.g., Wu et al., 2007), and in some regions, reconstructions are contradictory (e.g., de Vernal et al., 2006). For example, some LGM climate reconstructions suggest that the Iberian Peninsula was dry (Bartlein et al., 2011; Cleator et al., 2020), while others suggest wetter conditions were prevalent (Moreno et al., 2012). Some of these discrepancies may result from the fact that many paleoclimate archives record a certain season, while the signal is frequently interpreted as an annual value (Beghin et al., 2016), or because even sites that are close together record strong climatic gradients. Whatever the case, generation of a spatially continuous map of climate and environmental conditions in LGM Europe is currently not possible using a strictly data-driven approach. As an alternative, it should be possible to generate continuous maps using climate models.

GCM simulations are overall consistent with reconstructions in simulating an LGM climate that is largely colder and drier than present day (e.g., Ludwig et al., 2016; Hofer et al., 2012a). At the regional scale, however, GCMs show broad intermodel variety and partly disagree in comparison to proxy reconstructions, particularly concerning the magnitude and spatial patterning of temperature and precipitation (Harrison et al., 2015). For example, GCMs show broad disagreement in the simulation of precipitation over the Iberian Peninsula, with some models suggesting it was wetter while in others the simulated climate is drier (Beghin et al., 2016). One possible explanation for the disagreement is the coarse spatial resolution of the GCMs; at the continental scale, mountains, ice sheets, and water bodies have an important influence on regional circulation and climate that may not be represented appropriately at a typical GCM resolution of ca. 100 km (Stocker et al., 2013).

To improve the representation of local and regional climate, GCMs can be dynamically downscaled using regional climate models (RCMs). Ludwig et al. (2019) found that downscaling using an RCM offers a clear benefit to answer paleoclimate research questions and to improve interpretation of climate modelling and proxy reconstructions. They also found that the regional climate models require appropriate surface boundary conditions to properly represent the lower troposphere. Studies have demonstrated that a realistic representation of surface conditions is essential for the accuracy of the simulated regional climate as they play a crucial role in regulating water and energy fluxes between the land surface and the atmosphere (e.g., Crowley and Baum, 1997; Strandberg et al., 2011; Tao et al., 2013; Ludwig et al., 2017).

As noted above, the sparse distribution of paleoecological samples in Europe that are securely dated to the LGM preclude the development of a continuous map of land cover that can be used as a boundary condition for climate modelling and other purposes, e.g., archaeological and botanical research. Since climate affects land cover and land cover in turn affects climate , it is not sufficient to simply use climate model output to generate a vegetation map. To overcome this dichotomy, one may adopt a coupled modelling approach, where a climate model simulation is initialised with an estimate of land cover and the resulting climate output fields are used to simulate land cover. This process, which is called asynchronous coupling, is

https://doi.org/10.5194/cp-2020-147
Preprint. Discussion started: 21 November 2020


Climate of the Past Discussions

repeated between the climate and land cover models until the land-atmosphere system is in equilibrium. Asynchronous coupling is computationally inexpensive and has been successfully employed in several modelling studies to investigate problems in paleoclimate science (e.g., Texier et al., 1997; Noblet et al., 1996).

Here, we perform an asynchronous coupled modelling study to simulate the climate and land cover of Europe at the LGM. The coupled modelling starts with a GCM (CCSM4; Gent et al., 2011) to simulate global atmospheric boundary conditions, which are then passed to an RCM (WRF; Skamarock and Klemp, 2008). The RCM output is used to drive a dynamic vegetation model (LPJ-LMfire; Pfeiffer et al., 2013) which then returns land cover to the RCM. The RCM simulation is then repeated with the new land cover as boundary condition. We evaluate the results of our coupled model experiment using independent reconstructions of land cover and climate, and we perform sensitivity tests to better understand the importance of land cover for LGM climate in Europe by forcing the RCM with an alternative set of land-surface boundary conditions.

2 Models and methods

2.1 General circulation model: CCSM4

The atmosphere and land component of the Community Climate System Model (version 4; CCSM4; Gent et al., 2011) were used to perform two global climate simulations: 31 consecutive years for 1990 conditions and another 31 consecutive years for LGM conditions (Hofer et al., 2012a,b; Merz et al., 2013, 2014a,b, 2015). The atmospheric component (CAM4, Neale et al., 2010) and the land component (CLM4, Oleson et al., 2010) are coupled to so-called *data models* for the ocean and sea ice. This means that the atmospheric component is forced by time-varying sea surface temperatures and sea ice cover, deduced from a more coarsely resolved fully coupled simulation with CCSM3 (Hofer et al., 2012a). The atmosphere-land-only model is run with 6-hourly output, a horizontal resolution of 1.25 $^\circ$ $\times$ 0.9 $^\circ$ (longitude $\times$ latitude) and 26 vertical hybrid sigma-pressure levels.

2.2 Regional climate model: WRF

To investigate the importance of model resolution and land cover on the climate of LGM Europe, we dynamically downscaled the global CCSM4 simulations using the Weather Research and Forecasting (WRF) model (version 3.8.1, Skamarock and Klemp, 2008). This regional climate model was set up with two domains that are two-way nested. These domains have 40 vertical eta levels and a horizontal resolution of 56 and 18 km, respectively. The outermost domain is centered on the Alpine region and includes an extended westward and northward area to capture the influence of the North Atlantic Ocean and the Fennoscandian ice sheet on the European climate (Fig. 1). The relevant parameterisation schemes chosen to run WRF are described in Velasquez et al. (2020).

We performed three sets of WRF simulations for this study. Each simulation was run for 30 years, split up into two single 15-year simulations and carried out with an adaptive time-step to increase the throughput on the available computer facilities. For each of the 15-year simulations, we used a 2-month spin-up to account for the time required for the land surface to

https://doi.org/10.5194/cp-2020-147
Preprint. Discussion started: 21 November 2020


Climate of the Past Discussions

come into equilibrium. Tests show that the WRF land surface scheme reaches a quasi-equilibrium after approximately 15 days (Velasquez et al., 2020). The initial and boundary conditions for WRF were provided by the global CCSM4 simulations. Note that no nudging is applied in the RCM simulations. The main simulation (LGM_{LGM}) is the final product of our coupling design and uses the GCM simulation with perpetual LGM conditions (Hofer et al., 2012a). Reduced sea level and increased ice sheets are used for LGM conditions as specified in the PMIP3 protocol (for more details see: Hofer et al., 2012a; Ludwig et al., 2017). The LGM glaciation over the Alpine region is obtained from Seguinot et al. (2018) and additional LGM glaciated areas (e.g., Pyrenees, Carpathians) is from Ehlers et al. (2011). Calculation of the LGM land cover is described in Sect. 2.4.

We carried out two additional sensitivity simulations to evaluate the importance of land cover for the LGM climate in Europe and to gain insights into the atmospheric response to changes in land cover. Namely, the sensitivity simulations were compared against the final product of our coupling design (LGM_{LGM}). The first additional WRF simulation (PD_{PD}) is run using the GCM simulation with 1990 conditions (Hofer et al., 2012a), and uses the default present-day MODIS-based land cover dataset from WRF as the land surface boundary condition (Skamarock and Klemp, 2008). The second additional simulation uses the GCM simulation with LGM conditions (Hofer et al., 2012a), but with the default present-day MODIS-based land cover dataset from WRF as for the land surface (LGM_{PD}). Comparing LGM_{PD} with PD_{PD} illustrates the atmospheric response to changes only in the atmospheric forcing, i.e., without changes in land cover. The comparison of LGM_{LGM} and the LGM_{PD} allows us to extract the influence of land cover on the atmosphere, i.e., without changes in atmospheric boundary conditions. These simulations are summarised in Table 1.

2.3 Dynamic global vegetation model: LPJ-LMfire

Land cover for the LGM is simulated by the LPJ-LMfire dynamic global vegetation model (Pfeiffer et al., 2013), which is an evolution of LPJ (Sitch et al., 2003). LPJ-LMfire is a processed-based, large-scale representation of vegetation dynamics and land-atmosphere water and carbon exchanges that simulates land cover patterns in response to climate, soils, and atmospheric CO_2 concentrations (Prentice et al., 1992; Haxeltine and Prentice, 1996; Haxeltine et al., 1996; Kaplan, 2001; Kaplan et al., 2016). LPJ-LMfire simulates land cover in the form of the fractional coverage of nine plant functional types (PFTs), including tropical, temperate, and boreal trees, and tropical and extratropical herbaceous vegetation (Sitch et al., 2003).

In each of our simulations, we drove LPJ-LMfire for 1020 years with the climate from the GCM and RCM, reconstructed atmospheric CO_2 concentrations from ice cores, and present-day soil physical properties extrapolated out on to the continental shelves (Kaplan et al., 2016). Such a long simulation is not necessary to bring aboveground vegetation into equilibrium with climate, but it allows soil organic matter to equilibrate and because the vegetation model is computationally inexpensive, we performed these millennium-long simulations so that they could be analysed for other purposes in the future.

2.4 Iterative asynchronous coupling design

To create the best possible estimate of European land cover for the LGM, we used an iterative asynchronous coupling design that combines CCSM4/WRF with LPJ-LMfire model (i.e., LGM_{LGM}). This coupling design consists of four steps: (i) the fully coupled CCSM4 provides atmospheric variables for the LGM to generate the first approximation of LGM land cover with

https://doi.org/10.5194/cp-2020-147
Preprint. Discussion started: 21 November 2020


Climate of the Past Discussions

LPJ-LMfire at a horizontal resolution of 1.25 ° × 0.9 ° (longitude × latitude), (ii) WRF is driven by the CCSM4 with LGM conditions and the first approximation of LGM land cover created in step (i) to generate the first downscaled atmospheric variables for the LGM at 18 and 54 km resolution, (iii) LPJ-LMfire is run with the downscaled LGM atmospheric variables (from step ii) to regenerate the LGM land cover at the RCM resolutions, (iv) same as in (ii) but WRF uses the land surface boundary conditions simulated at 18 and 54 km. Step (iii) and (iv) are carried out asynchronously over six iterations to achieve a quasi-equilibrium between the climate and land cover. Parts (i) and (ii) are considered as the first iteration and the iterations of (iii) and (iv) are considered as the second-to-seventh iterations. The variables that are passed between the climate and vegetation models are summarised in Table 2. Note that to classify vegetation cover fraction into the land cover categories required by WRF (according to NOAH-MP MODIS; Niu et al., 2011), we used a simple scheme based only on the cover fraction of the LPJ-LMfire PFTs.

3 Effect of the iterative asynchronous coupling

The offline coupling design (Sect. 2.4) aims at generating a simulation of LGM climate and land cover that is as realistic as possible. Through empirical observation, we determined that the land surface and atmosphere were in quasi-equilibrium after seven iterations. To describe this result and its effects, we concentrate on the climate and land cover responses over the ice-free land areas of Europe at LGM. These responses are quantified throughout the iterations using variables that mostly govern the interaction between the atmosphere and land surface and thus, they are most suitable to illustrate the asynchronous coupling design and its performance. These variables are: the spatial climatological of total precipitation, temperature at 2 m and green vegetation fraction, and the number of grid points dominated by the following land cover categories: sparsely vegetated, tundra, forest, and shrublands (NOAH-MP MODIS categories, Niu et al., 2011). Land cover categories that are functionally similar are grouped together, e.g., wooded tundra, mixed tundra and barren tundra are all combined to the category tundra. Some land cover categories are not considered in our analysis as they are poorly represented in both periods, e.g., savanna, grassland and wetland, or are not relevant for the LGM, e.g., cropland and urban (Fig. 3a-b).

We observe that the most notable changes in the variables exchanged between land cover and atmosphere occur within the first four iterations (Fig. 2a,d). The variables level off from the fifth to the seventh iteration. In particular, we observe two sharp changes in all variables within the first four iterations. The first important change occurs between the first and second iteration and is observed in the atmospheric and land surface variables. This can be attributed to the important increase in the horizontal resolution from approximately 1 ° to 18 km, which can be explained by the better representation of the regional-to-local circulation processes and interactions with other components of the climate system in the RCM (Ludwig et al., 2019). The second change happens between the third and fourth iteration but is only observed in the atmospheric variables (Fig. 2a). Oscillations in spatial-averaged temperature at 2 m are observed in the first four iterations (maximum change of 0.5 °C), which turn into small fluctuations in the range of a tenth of a degree afterwards (Fig. 2a). The spatial-averaged total precipitation continuously decreases till the fourth iteration (drop of 13 mm) with small changes thereafter (increase of 4 mm; Fig. 2a). Changes in land surface variables are observed in the first three iterations and remain rather small thereafter, especially in the

https://doi.org/10.5194/cp-2020-147
Preprint. Discussion started: 21 November 2020


Climate of the Past Discussions

green vegetation fraction and the category sparsely vegetated (Fig. 2d). The small changes found after the fourth iteration are interpreted as internal variability in the models and therefore we assume that the quasi-equilibrium state is achieved after the fourth iteration.

In the following, we analyse the spatial patterns of climate and land cover between the iterations that represent the transient progression towards equilibrium (fourth minus first iteration) and the quasi-equilibrium state (seventh minus fourth iteration). We consider total precipitation and green vegetation fraction as variables that summarise the coupled land-atmosphere response. These two variables are displayed as relative changes with respect to the response of the fourth iteration (Fig. 2b-c and 2e-f). Precipitation during the transient state reveals a progressive wetting over the Iberian Peninsula, France and Balkan Peninsula, and drying over central and eastern Europe, north of the Alps and over some regions of France (Fig 2b). In response to the progressive changes in precipitation, the vegetation cover shows a strong decrease during the transient state, particularly in eastern Europe (over 80 % reduction, with respect to the fourth iteration) and the Italian Peninsula, and an increase over the Iberian Peninsula (around 40 %, with respect to the fourth iteration) and north of the Alps (around 60 %, with respect to the fourth iteration; Fig. 2e). Regions that experience a drying (wetting) are related to a reduction (an increase) in vegetation cover, except for the northern Alpine region. The changes in the quasi-equilibrium state are minimal for both variables (Fig. 2c and 2f). The remaining small differences could be interpreted as a part of the internal variability and uncertainties predominantly caused by parameterisations in the models, e.g., cloud formation and microphysical processes (Casanueva et al., 2016; Rajczak and Schär, 2017; Shrestha et al., 2017; Knist et al., 2018; Yang et al., 2019).

4 Comparison of the simulated land surface conditions to proxy reconstructions

To evaluate the $\mathrm{LGM}_{\mathrm{LGM}}$ climate and land cover simulations, we compare the simulated tree cover, land cover categories, temperature, and precipitation to pollen-based reconstructions. Reconstructed tree cover comes from the BIOME6000 pollen data synthesis (Prentice and Jolly, 2000) and a newer synthesis by Kaplan et al. (2016). For the land cover categories, temperature and precipitation, we use the 14 available pollen-based reconstructions for LGM Europe from Wu et al. (2007).

In the $\mathrm{PD}_{\mathrm{PD}}$ simulations, the land cover of Europe is principally composed of croplands and forests, while in the $\mathrm{LGM}_{\mathrm{LGM}}$ simulation land cover is dominated by sparsely vegetated and tundra categories (Fig. 4a and b). The $\mathrm{LGM}_{\mathrm{LGM}}$ simulation shows a large decrease in the total vegetation cover fraction compared to $\mathrm{PD}_{\mathrm{PD}}$ (comparing Fig. 3c to 3d). These changes are driven by lower temperatures and reduced precipitation, and lower global atmospheric CO_2 concentrations (Gerhart and Ward, 2010; Woillez et al., 2011; Chen et al., 2019; Lu et al., 2019). The $\mathrm{LGM}_{\mathrm{LGM}}$ land cover is in good agreement with the pollen-based reconstructions. We interpret the pollen reconstructions of steppe vegetation as sparsely vegetated in the WRF land cover categories (Niu et al., 2011). We use the nine nearest 18 km grid points surrounding each pollen site to compare the model results with pollen-based reconstructions of the land cover categories. For the land cover, the model-proxy agreement is considered to be good when at least one of the grid points matches the proxy reconstruction. For example, the dominant land cover category northwest of the Alps (47.73° N, 6.5° E) reconstructed from pollen (steppe) agrees with the surrounding

https://doi.org/10.5194/cp-2020-147
Preprint. Discussion started: 21 November 2020


Climate of the Past Discussions

simulated land cover (sparse vegetation). Over areas with few proxy reconstructions, e.g., Carpathian Basin, the modelled LGM land cover categories show tundra and grassland, which is in agreement with results found by Magyari et al. (2014a,b).

To assess the simulated $\mathrm{LGM}_{\mathrm{LGM}}$ climate, we calculate the temperature and precipitation anomalies with respect to $\mathrm{PD}_{\mathrm{PD}}$, i.e., model-based anomalies. These are then evaluated using anomalies from the pollen-based paleoclimate reconstructions. We extract the simulated climate for January and July as the reconstructions are only available for the coldest and warmest months. In general, cooler and drier anomalies are observed in the $\mathrm{LGM}_{\mathrm{LGM}}$ with especially pronounced cooling in January and drying in July (Fig. 4a-b and 4c-d). In January, we observe a positive precipitation anomaly of up to 7 mm day^{-1} over the Iberian Peninsula, northern Italy and the Dinaric Alps (Fig. 4c). In our model-proxy comparison of paleoclimate anomalies, we use only the nearest model grid point to the pollen site and consider the model and proxy reconstruction to agree when the model-based anomaly is within the 90 % confidence interval of the pollen-based anomaly (more details about the proxies in: Wu et al., 2007). The $\mathrm{LGM}_{\mathrm{LGM}}$ climate agrees with the pollen-based paleoclimate reconstructions at most sites.

Still, a few locations show considerable differences between the pollen-based and model-based climate anomalies, in line with similar findings mentioned in earlier studies (e.g.; Beghin et al., 2016; Ludwig et al., 2016; Cleator et al., 2020). These differences could be associated with shortcomings within the RCM and/or uncertainties in the proxy reconstructions (Bartlein et al., 2011; Ludwig et al., 2019; Cleator et al., 2020). Kageyama et al. (2006) suggested that terrestrial paleoclimate proxies may be more sensitive to climatic extremes than to the climatological mean state, which could lead to part of the discrepancies between pollen-based reconstructions and the model simulations. For example, there is large model-proxy disagreement in January precipitation over the Iberian Peninsula. Based on evidence for the presence of certain tree species in the northwestern part of the Iberian Peninsula, Roucoux et al. (2005) suggested that the LGM was not necessarily the period of the most severe, i.e., cold and dry, climatic conditions everywhere, with the LGM *sensu strictu* being warmer and wetter than preceding and following periods (Ludwig et al., 2018) . Similarly, Beghin et al. (2016) and Morellón et al. (2009) found evidence for the same wetter conditions in the interior and northwestern Iberian Peninsula. To explain these climate anomalies, studies have suggested that the North Atlantic storm track was shifted southward during the LGM compared to present day (e.g.; Hofer et al., 2012a; Luetscher et al., 2015; Merz et al., 2015; Ludwig et al., 2016; Wang et al., 2018; Raible et al., 2020). This could explain why the LGM simulations (i.e., $\mathrm{LGM}_{\mathrm{LGM}}$) shows wetter climate over the Iberian Peninsula compared to present-day conditions (i.e., $\mathrm{PD}_{\mathrm{PD}}$) in wintertime. Lofverstrom (2020) also proposed that stationary large-scale waves could have brought abundant precipitation to the western Mediterranean region (around 50 % of the total wintertime precipitation). It is important to note that we had only two pollen-based quantitative climate reconstructions from Iberia for the LGM; we therefore consider the model-proxy intercomparison in this region equivocal. In general, there is a good agreement between our simulations and the independent paleoclimate reconstructions.

We further evaluated the LPJ-LMfire simulations against inferred tree cover from 71 pollen sites across Europe containing samples securely dated to the LGM based on a compilation by Kaplan et al. (2016). This compilation represents a substantial improvement in spatial coverage and dating precision compared to the 14 sites of BIOME6000 used by Wu et al. (2007). Comparison between modelled and reconstructed tree cover is shown in Fig. 5. Generally, LPJ-LMfire moderately underestimates tree cover compared with the pollen-based reconstructions. Modelled tree cover has a maximum value of about 60 %, while

https://doi.org/10.5194/cp-2020-147
Preprint. Discussion started: 21 November 2020


Climate of the Past Discussions

there are eight sites where the reconstruction is $>$ 60 %, and two samples with 100 % tree cover. As noted by Kaplan et al. (2016), these sites with very high reconstructed tree cover fraction should be treated with caution because they may represent locations with very little vegetation, e.g., at the edge of the Alpine ice sheet or at high-altitude in the Carpathian Mountains. Therefore, the pollen signal is dominated by the long-distance transport of tree pollen; this phenomenon is also observed, e.g., in the analysis of pollen trapped in glacier ice (Brugger et al., 2019). At the bulk of the sites, LPJ-LMfire simulates 10-20 % lower tree cover than reconstructed by pollen, which is within the uncertainty of both datasets (Kaplan et al., 2016), but may suggest that the modelled climate is too cold and/or too dry, or that the LPJ-LMfire model is too sensitive to low atmospheric CO_2 concentrations.

5 Atmospheric sensitivity to land cover

To better understand the importance of the land surface for the LGM climate in Europe, we assess sensitivity simulations by comparing PD_{PD}, LGM_{PD} and LGM_{LGM}. Our assessment considers the land areas without snow/ice that are shared by both LGM and PD climate (crosshatched areas in Fig.6), i.e., we discard glaciated areas and land areas on the continental shelves that were exposed at the LGM. Again, temperature and precipitation are selected as main indicators of the atmospheric response. Comparing LGM_{LGM} to PD_{PD} shows a cooling of around -12 °C in the annual value (Table 3). This cooling is enhanced to -15.3 °C in DJF (December-January-February), remains similar to the annual mean in MAM and SON (March-April-May and September-October-November), and weakens to -7.2 °C in JJA (June-July-August; Table 3). Moreover, a precipitation decrease is noted in the annual value, which also applies to most months and in particular to JJA. Only in DJF, we observe a marginal increase in precipitation (Table 3). This clearly illustrates a seasonality in the atmospheric response. Broccoli and Manabe (1987) mentioned that one reason for the seasonality in the temperature response can be the fluctuations in the horizontal thermal advection from glaciers and ice-sheets to ice-free regions, predominantly in winter and weakened in summer (due to weaker winds and stronger solar radiation). Cao et al. (2019) on one hand attributed the overall decrease of precipitation to the strong anticyclonic circulations over the ice-sheets, especially to the low-level divergent cold air (Schaffernicht et al., 2020). On the other hand, Luetscher et al. (2015) and Lofverstrom (2020) attributed winter wetter conditions over Europe to atmospheric rivers and Rossby-wave breaking, respectively. This together with the southward shift of storm track (found by: Hofer et al., 2012a; Luetscher et al., 2015; Ludwig et al., 2016; Wang et al., 2018; Raible et al., 2020) could then compensate the general dryness in wintertime, which would therefore lead to the seasonality.

To investigate the origin of the atmospheric response of the LGM_{LGM} with respect to the PD_{PD}, we evaluate the atmospheric response to changes in the forcing (i.e., LGM_{PD} – PD_{PD}) and to changes in the land cover (i.e., LGM_{LGM} – LGM_{PD}), separately. The temperature response is clearly dominated by changes in the forcing, especially in SON and DJF. While changes in land cover can only slightly influence temperature by an additional cooling of 0.66 °C in MAM and a warming of 0.85 °C in JJA (Table 3). The precipitation anomaly is dominated by changes in the forcing as well. However, it is affected by changes in the land cover only in DJF and JJA where precipitation is reduced by about 43 % in DJF and enhanced by about 35 % in JJA. This demonstrates that the seasonality of the atmospheric response is mainly driven by changes in the forcing but its

https://doi.org/10.5194/cp-2020-147
Preprint. Discussion started: 21 November 2020


Climate of the Past Discussions

intensity can be modulated by changes in the land cover, in particular in the precipitation response. A possible reason for the seasonality in the response may be a modification of the stability in the lowest levels of the atmosphere that is produced by the changes in the land cover. A cooling (warming) in the lower layer may lead to an inversion (unstable) zone that therefore weakens (enhances) precipitation processes. Jahn et al. (2005) found that the LGM-like vegetation cover produces colder temperatures (ca. -0.6 °C globally), especially in areas with the greatest decrease in tree cover. Ludwig et al. (2017) suggested that including LGM-like vegetation into regional climate modeling causes changes in albedo, net radiation and heat fluxes that leads to impacts on temperature and precipitation. Another hypothesis is that the variability in land cover would lead to modifications in the evapotranspiration affecting the moisture recycling and thus the increases in precipitation (Wallace and Hobbs, 2006). This suggests that modifications in land cover like deforestation or growth of urban areas could play an important role when other forcing agents marginally change, as has been observed in some future climate change scenarios like RCP 2.6 and 4.5 (Stocker et al., 2013).

We further analysed the spatial pattern of the atmospheric response to changes in land cover ($\mathrm{LGM_{LGM}} - \mathrm{LGM_{PD}}$). To be consistent with the evaluation done in Sect. 4, we focus on temperature and precipitation in January and July. Annual mean temperature shows a cooling of around -2 °C in the vicinity of glaciers and in high-altitude regions; while warming is visible in lower-elevation areas including the southwestern part of the Iberian Peninsula, France and the Carpathian Basin. (Fig. 6a). A similar spatial pattern is observed in January and July: Stronger warming is especially noted in the northern part of Italy in January (Fig. 6b), whereas we observe that the amplitude of the temperature anomaly becomes stronger in July, especially where the positive temperature anomaly covers a larger area, e.g., over eastern Europe (Fig. 6c). The precipitation response is moderate in the annual mean. A slight increase of precipitation is seen in parts of the Mediterranean Sea and the Iberian Peninsula, while a general decrease is observed over the rest of Europe. An enhanced similar pattern is observed in January, but with a slight increase over Germany and eastern Europe. LGM land cover leads to a negative precipitation anomaly in July, which is especially strong around the Alps and in eastern Europe. Even though changes in land cover have a small-to-moderate effect on the temperature and precipitation response, respectively (Table 3), their spatial pattern strongly changes across Europe. Particularly, changes in land cover could be very important in some locations and seasons when we might expect the land-atmosphere coupling strength to be strong, such as eastern Europe in July.

6 Conclusions

In this study, we investigated the importance of land-atmosphere feedbacks for the climate of Europe during the Last Glacial Maximum. To this end, we performed a series of high-resolution asynchronously coupled atmosphere-vegetation modelling simulations. We simulated European climate and vegetation using the WRF regional climate model and LPJ-LMfire vegetation model on a 56 and an 18 km horizontal resolution.

Results of the asynchronous coupling show that quasi-equilibrium between climate and land cover is reached after the fourth iteration. Between the first and fourth iteration, the climate becomes progressively wetter in southern Europe, while it becomes drier in the east of the model domain. Once the coupled model system reaches equilibrium (from fourth to seventh iterations),

https://doi.org/10.5194/cp-2020-147
Preprint. Discussion started: 21 November 2020


Climate of the Past Discussions

we identified only marginal spatial differences that we attribute to internal variability in the climate and vegetation models. The final iteration of the asynchronous coupling represents our best estimate of the atmospheric and land surface conditions in Europe at LGM. Consistent with many previous studies, we observe that the LGM climate of Europe was generally much colder and drier compared to present day. The $\mathrm{LGM_{LGM}}$ land cover was characterised by tundra and sparse vegetation, although in many parts of central Europe open forest parkland may have been common, a result which is supported by comparisons with pollen-based vegetation reconstructions.

Using two additional sensitivity simulations: $\mathrm{PD_{PD}}$ and $\mathrm{LGM_{PD}}$, we quantified the direct effects of land cover on the LGM climate. Comparing $\mathrm{LGM_{LGM}}$ to $\mathrm{PD_{PD}}$ shows not only a general cooling and drying, but also illustrates a seasonality in the atmospheric response. This seasonality may be related to fluctuations in circulation patterns. Comparing $\mathrm{LGM_{PD}}$ to $\mathrm{PD_{PD}}$ illustrates that the seasonality is mainly driven by changes in forcing. Changes in land cover can however modify the intensity of the climatic response, especially for summer precipitation. The comparison between $\mathrm{LGM_{LGM}}$ to $\mathrm{LGM_{PD}}$ shows that, even in Europe where we would generally expect a weak land-atmosphere coupling compared, e.g., to the monsoon tropics, the atmosphere is sensitive to changes in land cover. The land-atmosphere response also has a seasonality which differs across Europe. These features can be partially explained by the variable spatial and temporal influence of vegetation cover (albedo) and water fluxes (partitioning of sensible vs. latent heat fluxes) to the lower troposphere. Our results show that LGM land cover led to more (less) pronounced dryness over central (eastern) Europe in summer (JJA) when influenced by a more (less) reduced vegetation cover fraction.

As more paleoenvironmental reconstructions become available in the future, these simulations will be worthy of further evaluation and more detailed examination of specific areas. Although 18 km is relatively high resolution for regional climate models, future studies benefit from even more detailed climate simulations, particularly to better understand precipitation patterns in complex terrain such as Iberia, across the Mediterranean, and in the Carpathians. This is also true for studies on the local and regional paleobotany and archaeology of this important period in Europe's history.

Code and data availability. WRF is a community model that can be downloaded from its web page (http://www2.mmm.ucar.edu/wrf/users/code_admin.php, last access 12 October 2020) (Skamarock and Klemp, 2008). The source code of LPJ-LMfire can be downloaded from Github (https://github.com/ARVE-Research/LPJ-LMfire/tree/v1.3, last access: 04 November 2020) (Kaplan et al., 2018). The climate simulations (global: CCSM4 and regional: WRF) and land cover simulations (LPJ-LMfire) occupy several terabytes and thus are not freely available. Nevertheless, they can be accessed upon request to the contributing authors. Simple calculations carried out at a grid point level are performed with Climate Data Operator (CDO, Schulzweida, 2019) and NCAR Command Language (NCL, UCAR/NCAR/CISL/TDD, 2019). The figures are performed with NCL (UCAR/NCAR/CISL/TDD, 2019). Source code of the program to classify vegetation cover fraction into the WRF land cover categories is archived on Github (https://github.com/ARVE-Research/lpj2wrf).

https://doi.org/10.5194/cp-2020-147
Preprint. Discussion started: 21 November 2020

Climate of the Past Discussions

Author contributions. PV, JOK, and CCR contributed to the design of the experiments. PV carried out the climate simulations and wrote the first draft. JOK carried out the land cover simulations. P.L. provided the guidelines for introducing new land-cover conditions into WRF. M.M. provided support in the application of these guidelines. All authors contributed to the writing and scientific discussion.

Competing interests. The authors declare no competing interests.

Acknowledgements. This work was supported by the Swiss National Science Foundation (SNF) within the project 'Modelling the ice flow in the western Alps during the last glacial cycle' (grant: 200021-162444). JOK is grateful for computing support from the School of Geography, University of Oxford. The simulations are performed on the super computing architecture of the Swiss National Supercomputing Centre (CSCS). PL thanks the Helmholtz initiative REKLIM for funding. MM is supported by the Early Postdoc.Mobility program (SNF, grant: P2BEP_181837). Data is locally stored on the oschgerstore provided by the Oeschger Center for Climate Change Research (OCCR).

https://doi.org/10.5194/cp-2020-147
Preprint. Discussion started: 21 November 2020

Climate of the Past Discussions

References

Baena Preysler, J., Carrión Santafé, E., Torres Navas, C., and Vaquero Rodríguez, M.: Mousterian inside the upper Paleolithic? The last interval of El Esquilleu (Cantabria, Spain) sequence, Quaternary International, 508, 153–163, https://doi.org/10.1016/j.quaint.2018.11.015, 2019.

Bartlein, P. J., Harrison, S. P., Brewer, S., Connor, S., Davis, B. A. S., Gajewski, K., Guiot, J., Harrison-Prentice, T. I., Henderson, A., Peyron, O., Prentice, I. C., Scholze, M., Seppä, H., Shuman, B., Sugita, S., Thompson, R. S., Viau, A. E., Williams, J., and Wu, H.: Pollen-based continental climate reconstructions at 6 and 21 ka: a global synthesis, Climate Dynamics, 37, 775–802, https://doi.org/10.1007/s00382-010-0904-1, 2011.

Beghin, P., Charbit, S., Kageyama, M., Combourieu-Nebout, N., Hatté, C., Dumas, C., and Peterschmitt, J.-Y.: What drives LGM precipitation over the western Mediterranean? A study focused on the Iberian Peninsula and northern Morocco, Climate Dynamics, 46, 2611–2631, https://doi.org/10.1007/s00382-015-2720-0, 2016.

Braconnot, P., Harrison, S. P., Kageyama, M., Bartlein, P. J., Masson-Delmotte, V., Abe-Ouchi, A., Otto-Bliesner, B., and Zhao, Y.: Evaluation of climate models using palaeoclimatic data, Nature Climate Change, 2, 417–424, https://doi.org/10.1038/nclimate1456, number: 6 Publisher: Nature Publishing Group, 2012.

Broccoli, A. J. and Manabe, S.: The influence of continental ice, atmospheric CO2, and land albedo on the climate of the last glacial maximum, Climate Dynamics, 1, 87–99, https://doi.org/10.1007/BF01054478, 1987.

Brugger, S. O., Gobet, E., Blunier, T., Morales-Molino, C., Lotter, A. F., Fischer, H., Schwikowski, M., and Tinner, W.: Palynological insights into global change impacts on Arctic vegetation, fire, and pollution recorded in Central Greenland ice, The Holocene, 29, 1189–1197, https://doi.org/10.1177/0959683619838039, 2019.

Burke, A., Levavasseur, G., James, P. M. A., Guiducci, D., Izquierdo, M. A., Bourgeon, L., Kageyama, M., Ramstein, G., and Vrac, M.: Exploring the impact of climate variability during the Last Glacial Maximum on the pattern of human occupation of Iberia, Journal of Human Evolution, 73, 35–46, https://doi.org/10.1016/j.jhevol.2014.06.003, 2014.

Cao, J., Wang, B., and Liu, J.: Attribution of the Last Glacial Maximum climate formation, Climate Dynamics, 53, 1661–1679, https://doi.org/10.1007/s00382-019-04711-6, 2019.

Casanueva, A., Kotlarski, S., Herrera, S., Fernández, J., Gutiérrez, J. M., Boberg, F., Colette, A., Christensen, O. B., Goergen, K., Jacob, D., Keuler, K., Nikulin, G., Teichmann, C., and Vautard, R.: Daily precipitation statistics in a EURO-CORDEX RCM ensemble: Added value of raw and bias-corrected high-resolution simulations, Climate Dynamics, 47, 719–737, https://doi.org/10.1007/s00382-015-2865-x, 2016.

Chen, W., Zhu, D., Ciais, P., Huang, C., Viovy, N., and Kageyama, M.: Response of vegetation cover to CO2 and climate changes between Last Glacial Maximum and pre-industrial period in a dynamic global vegetation model, Quaternary Science Reviews, 218, 293–305, https://doi.org/10.1016/j.quascirev.2019.06.003, 2019.

Clark, P. U., Dyke, A. S., Shakun, J. D., Carlson, A. E., Clark, J., Wohlfarth, B., Mitrovica, J. X., Hostetler, S. W., and McCabe, A. M.: The Last Glacial Maximum, Science, 325, 710–714, https://doi.org/10.1126/science.1172873, 2009.

Cleator, S. F., Harrison, S. P., Nichols, N. K., Prentice, I. C., and Roulstone, I.: A new multivariable benchmark for Last Glacial Maximum climate simulations, Climate of the Past, 16, 699–712, https://doi.org/10.5194/cp-16-699-2020, publisher: Copernicus GmbH, 2020.

Crowley, T. J. and Baum, S. K.: Effect of vegetation on an ice-age climate model simulation, Journal of Geophysical Research: Atmospheres, 102, 16 463–16 480, https://doi.org/10.1029/97JD00536, 1997.

https://doi.org/10.5194/cp-2020-147
Preprint. Discussion started: 21 November 2020

de Vernal, A., Rosell-Melé, A., Kucera, M., Hillaire-Marcel, C., Eynaud, F., Weinelt, M., Dokken, T., and Kageyama, M.: Comparing proxies for the reconstruction of LGM sea-surface conditions in the northern North Atlantic, Quaternary Science Reviews, 25, 2820–2834, https://doi.org/10.1016/j.quascirev.2006.06.006, 2006.

Ehlers, J., Gibbard, P., and Hughes, P.: Quaternary glaciations-extent and chronology: a closer look, vol. 15, Elsevier, Amsterdam, Netherlands, 2011.

Finlayson, C.: Neanderthals and modern humans: an ecological and evolutionary perspective, vol. 38, Cambridge University Press, 2004.

Finlayson, C.: On the importance of coastal areas in the survival of Neanderthal populations during the Late Pleistocene, Quaternary Science Reviews, 27, 2246–2252, https://doi.org/10.1016/j.quascirev.2008.08.033, 2008.

Finlayson, C., Giles Pacheco, F., Rodríguez-Vidal, J., Fa, D. A., María Gutierrez López, J., Santiago Pérez, A., Finlayson, G., Allue, E., Baena Preysler, J., Cáceres, I., Carrión, J. S., Fernández Jalvo, Y., Gleed-Owen, C. P., Jimenez Espejo, F. J., López, P., Antonio López Sáez, J., Antonio Riquelme Cantal, J., Sánchez Marco, A., Giles Guzman, F., Brown, K., Fuentes, N., Valarino, C. A., Villalpando, A., Stringer, C. B., Martinez Ruiz, F., and Sakamoto, T.: Late survival of Neanderthals at the southernmost extreme of Europe, Nature, 443, 850–853, https://doi.org/10.1038/nature05195, 2006.

Gent, P. R., Danabasoglu, G., Donner, L. J., Holland, M. M., Hunke, E. C., Jayne, S. R., Lawrence, D. M., Neale, R. B., Rasch, P. J., Vertenstein, M., Worley, P. H., Yang, Z.-L., and Zhang, M.: The Community Climate System Model Version 4, Journal of Climate, 24, 4973–4991, https://doi.org/10.1175/2011JCLI4083.1, 2011.

Gerhart, L. M. and Ward, J. K.: Plant responses to low [CO2] of the past, New Phytologist, 188, 674–695, https://doi.org/10.1111/j.1469-8137.2010.03441.x, 2010.

Harrison, S. P., Bartlein, P. J., Izumi, K., Li, G., Annan, J., Hargreaves, J., Braconnot, P., and Kageyama, M.: Evaluation of CMIP5 palaeo-simulations to improve climate projections, Nature Climate Change, 5, 735–743, https://doi.org/10.1038/nclimate2649, number: 8 Publisher: Nature Publishing Group, 2015.

Haxeltine, A. and Prentice, I. C.: BIOME3: An equilibrium terrestrial biosphere model based on ecophysiological constraints, resource availability, and competition among plant functional types, Global biogeochemical cycles, 10, 693–709, tex.publisher: Wiley Online Library, 1996.

Haxeltine, A., Prentice, I. C., and Creswell, I. D.: A coupled carbon and water flux model to predict vegetation structure, Journal of Vegetation Science, 7, 651–666, https://doi.org/10.2307/3236377, _eprint: https://onlinelibrary.wiley.com/doi/pdf/10.2307/3236377, 1996.

Hofer, D., Raible, C. C., Dehnert, A., and Kuhlemann, J.: The impact of different glacial boundary conditions on atmospheric dynamics and precipitation in the North Atlantic region, Climate of the Past, 8, 935–949, https://doi.org/10.5194/cp-8-935-2012, 2012a.

Hofer, D., Raible, C. C., Merz, N., Dehnert, A., and Kuhlemann, J.: Simulated winter circulation types in the North Atlantic and European region for preindustrial and glacial conditions: Glacial circulation types, Geophysical Research Letters, 39, https://doi.org/10.1029/2012GL052296, 2012b.

Jahn, A., Claussen, M., Ganopolski, A., and Brovkin, V.: Quantifying the effect of vegetation dynamics on the climate of the Last Glacial Maximum, Climate of the Past, 1, 1–7, https://doi.org/https://doi.org/10.5194/cp-1-1-2005, publisher: Copernicus GmbH, 2005.

Janská, V., Jiménez-Alfaro, B., Chytrý, M., Divíšek, J., Anenkhonov, O., Korolyuk, A., Lashchinskyi, N., and Culek, M.: Palaeodistribution modelling of European vegetation types at the Last Glacial Maximum using modern analogues from Siberia: Prospects and limitations, Quaternary Science Reviews, 159, 103–115, https://doi.org/10.1016/j.quascirev.2017.01.011, 2017.

Jia, K., Ruan, Y., Yang, Y., and Zhang, C.: Assessing the Performance of CMIP5 Global Climate Models for Simulating Future Precipitation Change in the Tibetan Plateau, Water, 11, 1771, https://doi.org/10.3390/w11091771, 2019.

https://doi.org/10.5194/cp-2020-147
Preprint. Discussion started: 21 November 2020

Kageyama, M., Laîné, A., Abe-Ouchi, A., Braconnot, P., Cortijo, E., Crucifix, M., de Vernal, A., Guiot, J., Hewitt, C. D., Kitoh, A., Kucera, M., Marti, O., Ohgaito, R., Otto-Bliesner, B., Peltier, W. R., Rosell-Melé, A., Vettoretti, G., Weber, S. L., and Yu, Y.: Last Glacial Maximum temperatures over the North Atlantic, Europe and western Siberia: a comparison between PMIP models, MARGO sea–surface temperatures and pollen-based reconstructions, Quaternary Science Reviews, 25, 2082–2102, https://doi.org/10.1016/j.quascirev.2006.02.010, 2006.

Kageyama, M., Albani, S., Braconnot, P., Harrison, S. P., Hopcroft, P. O., Ivanovic, R. F., Lambert, F., Marti, O., Peltier, W. R., Peterschmitt, J.-Y., Roche, D. M., Tarasov, L., Zhang, X., Brady, E. C., Haywood, A. M., LeGrande, A. N., Lunt, D. J., Mahowald, N. M., Mikolajewicz, U., Nisancioglu, K. H., Otto-Bliesner, B. L., Renssen, H., Tomas, R. A., Zhang, Q., Abe-Ouchi, A., Bartlein, P. J., Cao, J., Li, Q., Lohmann, G., Ohgaito, R., Shi, X., Volodin, E., Yoshida, K., Zhang, X., and Zheng, W.: The PMIP4 contribution to CMIP6 – Part 4: Scientific objectives and experimental design of the PMIP4-CMIP6 Last Glacial Maximum experiments and PMIP4 sensitivity experiments, Geoscientific Model Development, 10, 4035–4055, https://doi.org/https://doi.org/10.5194/gmd-10-4035-2017, publisher: Copernicus GmbH, 2017.

Kageyama, M., Harrison, S. P., Kapsch, M.-L., Löfverström, M., Lora, J. M., Mikolajewicz, U., Sherriff-Tadano, S., Vadsaria, T., Abe-Ouchi, A., Bouttes, N., Chandan, D., LeGrande, A. N., Lhardy, F., Lohmann, G., Morozova, P. A., Ohgaito, R., Peltier, W. R., Quiquet, A., Roche, D. M., Shi, X., Schmittner, A., Tierney, J. E., and Volodin, E.: The PMIP4-CMIP6 Last Glacial Maximum experiments: preliminary results and comparison with the PMIP3-CMIP5 simulations, Climate of the Past Discussions, pp. 1–37, https://doi.org/https://doi.org/10.5194/cp-2019-169, publisher: Copernicus GmbH, 2020.

Kaplan, J. O.: Geophysical Applications of Vegetation Modeling, library Catalog: infoscience.epfl.ch Number: THESIS_LIB Publisher: Lund University, 2001.

Kaplan, J. O., Pfeiffer, M., Kolen, J. C. A., and Davis, B. A. S.: Large scale anthropogenic reduction of forest cover in Last Glacial Maximum Europe, PLOS ONE, 11, e0166 726, https://doi.org/10.1371/journal.pone.0166726, 2016.

Kaplan, J. O., Pfeiffer, M., and Chaste, E.: ARVE-Research/LPJ-LMfire: LPJ-LMfire, https://doi.org/10.5281/zenodo.1184589, 2018.

Knist, S., Goergen, K., and Simmer, C.: Evaluation and projected changes of precipitation statistics in convection-permitting WRF climate simulations over Central Europe, Climate Dynamics, https://doi.org/10.1007/s00382-018-4147-x, 2018.

Lofverstrom, M.: A dynamic link between high-intensity precipitation events in southwestern North America and Europe at the Last Glacial Maximum, Earth and Planetary Science Letters, 534, 116 081, https://doi.org/10.1016/j.epsl.2020.116081, 2020.

Lu, Z., Miller, P. A., Zhang, Q., Wårlind, D., Nieradzik, L., Sjolte, J., Li, Q., and Smith, B.: Vegetation pattern and terrestrial carbon variation in past warm and cold climates, Geophysical Research Letters, 46, 8133–8143, https://doi.org/10.1029/2019GL083729, 2019.

Ludwig, P., Schaffernicht, E. J., Shao, Y., and Pinto, J. G.: Regional atmospheric circulation over Europe during the Last Glacial Maximum and its links to precipitation, Journal of Geophysical Research: Atmospheres, 121, 2130–2145, https://doi.org/10.1002/2015JD024444, 2016.

Ludwig, P., Pinto, J. G., Raible, C. C., and Shao, Y.: Impacts of surface boundary conditions on regional climate model simulations of European climate during the Last Glacial Maximum, Geophysical Research Letters, 44, 5086–5095, https://doi.org/10.1002/2017GL073622, 2017.

Ludwig, P., Shao, Y., Kehl, M., and Weniger, G.-C.: The Last Glacial Maximum and Heinrich event I on the Iberian Peninsula: A regional climate modelling study for understanding human settlement patterns, Global and Planetary Change, 170, 34–47, https://doi.org/10.1016/j.gloplacha.2018.08.006, 2018.

Ludwig, P., Gómez-Navarro, J. J., Pinto, J. G., Raible, C. C., Wagner, S., and Zorita, E.: Perspectives of regional paleoclimate modeling, Annals of the New York Academy of Sciences, 1436, 54–69, https://doi.org/10.1111/nyas.13865, 2019.

https://doi.org/10.5194/cp-2020-147
Preprint. Discussion started: 21 November 2020

Ludwig, P., Gavrilov, M. B., Markovic, S. B., Ujvari, G., and Lehmkuhl, F.: Simulated regional dust cycle in the Carpathian Basin and the Adriatic Sea region during the Last Glacial Maximum, Quaternary International, https://doi.org/10.1016/j.quaint.2020.09.048, 2020.

Luetscher, M., Boch, R., Sodemann, H., Spötl, C., Cheng, H., Edwards, R. L., Frisia, S., Hof, F., and Müller, W.: North Atlantic storm track changes during the Last Glacial Maximum recorded by Alpine speleothems, Nature Communications, 6, 6344, https://doi.org/10.1038/ncomms7344, number: 1 Publisher: Nature Publishing Group, 2015.

Magyari, E. K., Kuneš, P., Jakab, G., Sümegi, P., Pelánková, B., Schäbitz, F., Braun, M., and Chytrý, M.: Late Pleniglacial vegetation in eastern-central Europe: are there modern analogues in Siberia?, Quaternary Science Reviews, 95, 60–79, https://doi.org/10.1016/j.quascirev.2014.04.020, 2014a.

Magyari, E. K., Veres, D., Wennrich, V., Wagner, B., Braun, M., Jakab, G., Karátson, D., Pál, Z., Ferenczy, G., St-Onge, G., Rethemeyer, J., Francois, J. P., von Reumont, F., and Schäbitz, F.: Vegetation and environmental responses to climate forcing during the Last Glacial Maximum and deglaciation in the East Carpathians: attenuated response to maximum cooling and increased biomass burning, Quaternary Science Reviews, 106, 278–298, https://doi.org/10.1016/j.quascirev.2014.09.015, 2014b.

Maier, A., Lehmkuhl, F., Ludwig, P., Melles, M., Schmidt, I., Shao, Y., Zeeden, C., and Zimmermann, A.: Demographic estimates of hunter–gatherers during the Last Glacial Maximum in Europe against the background of palaeoenvironmental data, Quaternary International, 425, 49–61, https://doi.org/10.1016/j.quaint.2016.04.009, 2016.

Merz, N., Raible, C. C., Fischer, H., Varma, V., Prange, M., and Stocker, T. F.: Greenland accumulation and its connection to the large-scale atmospheric circulation in ERA-Interim and paleoclimate simulations, Climate of the Past, 9, 2433–2450, https://doi.org/10.5194/cp-9-2433-2013, 2013.

Merz, N., Born, A., Raible, C. C., Fischer, H., and Stocker, T. F.: Dependence of Eemian Greenland temperature reconstructions on the ice sheet topography, Climate of the Past, 10, 1221–1238, https://doi.org/10.5194/cp-10-1221-2014, 2014a.

Merz, N., Gfeller, G., Born, A., Raible, C. C., Stocker, T. F., and Fischer, H.: Influence of ice sheet topography on Greenland precipitation during the Eemian interglacial, Journal of Geophysical Research: Atmospheres, 119, 10,749–10,768, https://doi.org/10.1002/2014JD021940, 2014b.

Merz, N., Raible, C. C., and Woollings, T.: North Atlantic Eddy-Driven jet in interglacial and glacial winter climates, Journal of Climate, 28, 3977–3997, https://doi.org/10.1175/JCLI-D-14-00525.1, 2015.

Mix, A. C., Bard, E., and Schneider, R.: Environmental processes of the ice age: land, oceans, glaciers (EPILOG), Quaternary Science Reviews, 20, 627–657, https://doi.org/10.1016/S0277-3791(00)00145-1, 2001.

Morellón, M., Valero-Garcés, B., Anselmetti, F., Ariztegui, D., Schnellmann, M., Moreno, A., Mata, P., Rico, M., and Corella, J. P.: Late Quaternary deposition and facies model for karstic Lake Estanya (North-eastern Spain), Sedimentology, 56, 1505–1534, https://doi.org/10.1111/j.1365-3091.2008.01044.x, 2009.

Moreno, A., González-Sampériz, P., Morellón, M., Valero-Garcés, B. L., and Fletcher, W. J.: Northern Iberian abrupt climate change dynamics during the last glacial cycle: A view from lacustrine sediments, Quaternary Science Reviews, 36, 139–153, https://doi.org/10.1016/j.quascirev.2010.06.031, 2012.

Neale, R. B., Richter, J. H., Conley, A. J., Park, S., Lauritzen, P. H., Gettelman, A., Rasch, P. J., and Vavrus, J.: Description of the NCAR community atmosphere model (CAM4), National Center for Atmospheric Research Tech. Rep. NCAR/TN+ STR, http://www.cesm.ucar.edu/models/ccsm4.0/cam/docs/description/cam4_desc.pdf, 2010.

https://doi.org/10.5194/cp-2020-147
Preprint. Discussion started: 21 November 2020

Niu, G.-Y., Yang, Z.-L., Mitchell, K. E., Chen, F., Ek, M. B., Barlage, M., Kumar, A., Manning, K., Niyogi, D., Rosero, E., Tewari, M., and Xia, Y.: The community Noah land surface model with multiparameterization options (Noah-MP): 1. Model description and evaluation with local-scale measurements, Journal of Geophysical Research: Atmospheres, 116, https://doi.org/10.1029/2010JD015139, 2011.

Noblet, N. I. d., Prentice, I. C., Joussaume, S., Texier, D., Botta, A., and Haxeltine, A.: Possible role of atmosphere-biosphere interactions in triggering the Last Glaciation, Geophysical Research Letters, 23, 3191–3194, https://doi.org/10.1029/96GL03004, 1996.

Oleson, W., Lawrence, M., Bonan, B., Flanner, G., Kluzek, E., Lawrence, J., Levis, S., Swenson, C., Thornton, E., Dai, A., Decker, M., Dickinson, R., Feddema, J., Heald, L., Hoffman, F., Lamarque, J.-F., Mahowald, N., Niu, G.-Y., Qian, T., Randerson, J., Running, S., Sakaguchi, K., Slater, A., Stockli, R., Wang, A., Yang, Z.-L., Zeng, X., and Zeng, X.: Technical description of version 4.0 of the community land model (CLM), NCAR Technical Note NCAR/TN-478+STR, National Center for Atmospheric Research, Boulder, CO, Boulder, CO, http://www.cesm.ucar.edu/models/cesm1.0/clm/CLM4_Tech_Note.pdf, national Center for Atmospheric Research, Boulder, CO, 2010.

Pfeiffer, M., Spessa, A., and Kaplan, J. O.: A model for global biomass burning in preindustrial time: LPJ-LMfire (v1.0), Geoscientific Model Development, 6, 643–685, https://doi.org/10.5194/gmd-6-643-2013, 2013.

Prentice, I. C. and Jolly, D.: Mid-Holocene and glacial-maximum vegetation geography of the northern continents and Africa, Journal of Biogeography, 27, 507–519, https://doi.org/10.1046/j.1365-2699.2000.00425.x, 2000.

Prentice, I. C., Cramer, W., Harrison, S. P., Leemans, R., Monserud, R. A., and Solomon, A. M.: Special Paper: A Global Biome Model Based on Plant Physiology and Dominance, Soil Properties and Climate, Journal of Biogeography, 19, 117–134, https://doi.org/10.2307/2845499, publisher: Wiley, 1992.

Raible, C. C., Pinto, J. G., Ludwig, P., and Messmer, M.: A review of past changes in extratropical cyclones in the northern hemisphere and what can be learned for the future, Wiley Interdisciplinary Reviews: Climate Change, p. e680, https://doi.org/https://doi.org/10.1002/wcc.680, 2020.

Rajczak, J. and Schär, C.: Projections of future precipitation extremes over Europe: A multimodel assessment of climate simulations, Journal of Geophysical Research: Atmospheres, 122, 10,773–10,800, https://doi.org/10.1002/2017JD027176, 2017.

Roucoux, K. H., de Abreu, L., Shackleton, N. J., and Tzedakis, P. C.: The response of NW Iberian vegetation to North Atlantic climate oscillations during the last 65kyr, Quaternary Science Reviews, 24, 1637–1653, https://doi.org/10.1016/j.quascirev.2004.08.022, 2005.

Schaffernicht, E. J., Ludwig, P., and Shao, Y.: Linkage between dust cycle and loess of the Last Glacial Maximum in Europe, Atmospheric Chemistry and Physics, 20, 4969–4986, https://doi.org/10.5194/acp-20-4969-2020, 2020.

Schulzweida, U.: CDO User Guide (Version 1.9.6), https://doi.org/10.5281/zenodo.2558193, 2019.

Seguinot, J., Ivy-Ochs, S., Jouvet, G., Huss, M., Funk, M., and Preusser, F.: Modelling last glacial cycle ice dynamics in the Alps, The Cryosphere, 12, 3265–3285, https://doi.org/10.5194/tc-12-3265-2018, 2018.

Shrestha, R. K., Connolly, P. J., and Gallagher, M. W.: Sensitivity of WRF Cloud Microphysics to Simulations of a Convective Storm Over the Nepal Himalayas, The Open Atmospheric Science Journal, 11, https://doi.org/10.2174/1874282301711010029, 2017.

Sitch, S., Smith, B., Prentice, I. C., Arneth, A., Bondeau, A., Cramer, W., Kaplan, J. O., Levis, S., Lucht, W., Sykes, M. T., Thonicke, K., and Venevsky, S.: Evaluation of ecosystem dynamics, plant geography and terrestrial carbon cycling in the LPJ dynamic global vegetation model, Global Change Biology, 9, 161–185, https://doi.org/10.1046/j.1365-2486.2003.00569.x, 2003.

Skamarock, W. C. and Klemp, J. B.: A time-split nonhydrostatic atmospheric model for weather research and forecasting applications, Journal of Computational Physics, 227, 3465–3485, https://doi.org/10.1016/j.jcp.2007.01.037, 2008.

https://doi.org/10.5194/cp-2020-147
Preprint. Discussion started: 21 November 2020

Stocker, T., Plattner, G.-K., Tignor, M., Allen, S., Boschung, J., Nauels, A., Xia, Y., Bex, V., and Midgley, P., eds.: Climate change 2013: The physical science basis. Contribution of working group I to the fifth assessment report of IPCC the Intergovernmental Panel on Climate Change, Cambridge University Press, Cambridge, United Kingdom and New York, NY, USA, doi:10.1017/CBO9781107415324, 2013.

Strandberg, G., Brandefelt, J., Kjellstro M., E., and Smith, B.: High-resolution regional simulation of Last Glacial Maximum climate in Europe, Tellus A: Dynamic Meteorology and Oceanography, 63, 107–125, https://doi.org/10.1111/j.1600-0870.2010.00485.x, 2011.

Tao, Z., Santanello, J. A., Chin, M., Zhou, S., Tan, Q., Kemp, E. M., and Peters-Lidard, C. D.: Effect of land cover on atmospheric processes and air quality over the continental United States – a NASA unified WRF (NU-WRF) model study, Atmospheric Chemistry and Physics Discussions, 13, 5429–5475, https://doi.org/10.5194/acpd-13-5429-2013, 2013.

Texier, D., de Noblet, N., Harrison, S. P., Haxeltine, A., Jolly, D., Joussaume, S., Laarif, F., Prentice, I. C., and Tarasov, P.: Quantifying the role of biosphere-atmosphere feedbacks in climate change: coupled model simulations for 6000 years BP and comparison with palaeodata for northern Eurasia and northern Africa, Climate Dynamics, 13, 865–881, https://doi.org/10.1007/s003820050202, 1997.

UCAR/NCAR/CISL/TDD: The NCAR Command Language (Version 6.6.2) [Software], 10.5065/D6WD3XH5, 2019.

Van Meerbeeck, C. J., Renssen, H., and Roche, D. M.: How did Marine Isotope Stage 3 and Last Glacial Maximum climates differ? – Perspectives from equilibrium simulations, Climate of the Past, 5, 33–51, https://doi.org/https://doi.org/10.5194/cp-5-33-2009, 2009.

Velasquez, P., Messmer, M., and Raible, C. C.: A new bias-correction method for precipitation over complex terrain suitable for different climate states: a case study using WRF (version 3.8.1), Geoscientific Model Development, 13, 5007–5027, https://doi.org/doi.org/10.5194/gmd-13-5007-2020, 2020.

Wallace, J. M. and Hobbs, P. V.: Atmospheric science: an introductory survey, vol. 92, Elsevier, 2006.

Walsh, J. E., Chapman, W. L., Romanovsky, V., Christensen, J. H., and Stendel, M.: Global Climate Model Performance over Alaska and Greenland, Journal of Climate, 21, 6156–6174, https://doi.org/10.1175/2008JCLI2163.1, 2008.

Wang, N., Jiang, D., and Lang, X.: Northern Westerlies during the Last Glacial Maximum: Results from CMIP5 Simulations, Journal of Climate, 31, 1135–1153, https://doi.org/10.1175/JCLI-D-17-0314.1, 2018.

Woillez, M., Kageyama, M., Krinner, G., Noblet-Ducoudré, N. d., Viovy, N., and Mancip, M.: Impact of CO2 and climate on the Last Glacial Maximum vegetation: results from the ORCHIDEE/IPSL models, Climate of the Past, 7, 557–577, https://doi.org/10.5194/cp-7-557-2011, 2011.

Wu, H., Guiot, J., Brewer, S., and Guo, Z.: Climatic changes in Eurasia and Africa at the last glacial maximum and mid-Holocene: reconstruction from pollen data using inverse vegetation modelling, Climate Dynamics, 29, 211–229, https://doi.org/10.1007/s00382-007-0231-3, 2007.

Yang, Q., Dai, Q., Han, D., Chen, Y., and Zhang, S.: Sensitivity analysis of raindrop size distribution parameterizations in WRF rainfall simulation, Atmospheric Research, 228, 1–13, https://doi.org/10.1016/j.atmosres.2019.05.019, 2019.

Yokoyama, Y., Lambeck, K., De Deckker, P., Johnston, P., and Fifield, L. K.: Timing of the Last Glacial Maximum from observed sea-level minima, Nature, 406, 713–716, https://doi.org/10.1038/35021035, 2000.

https://doi.org/10.5194/cp-2020-147
Preprint. Discussion started: 21 November 2020

Climate of the Past Discussions
Open Access
EGU

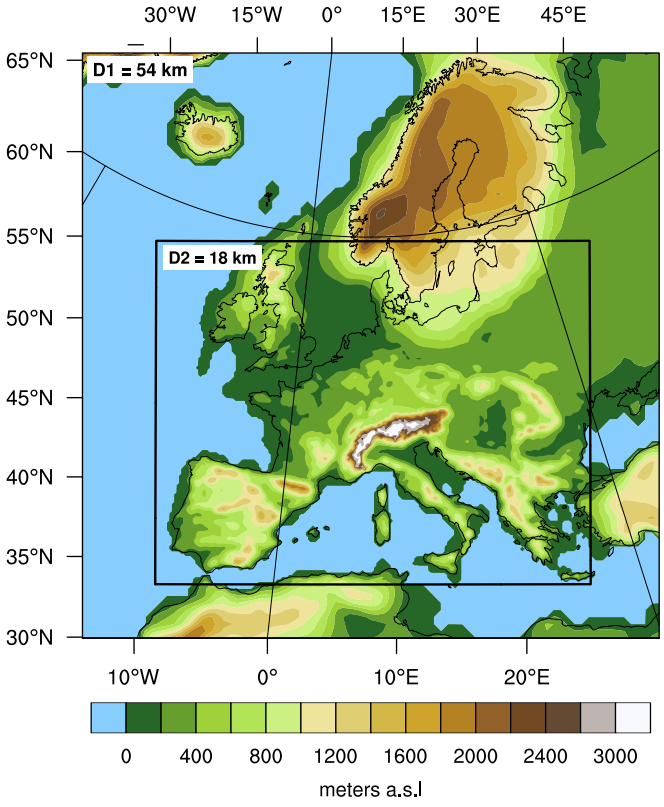

Figure 1. Topography and the two domains used by WRF for the LGM simulations.

https://doi.org/10.5194/cp-2020-147
Preprint. Discussion started: 21 November 2020

Climate of the Past Discussions
Open Access
EGU

Table 1. Set of simulations used in the asynchronous coupling and sensitivity experiments. First column indicates the name of the simulation, second and third columns the forcing used in the global and regional climate models, and fourth column the purpose of the comparison.

Name	**GCM simulations**	**RCM simulations**		**Aim**	
	(Hofer et al. 2012a)	topography and other forcing	land cover	insights into the responses to changes in the:	
PD_{PD}	1990s	1990s	1990s	forcing	
LGM_{PD}	LGM	LGM	1990s		land cover
LGM_{LGM}	LGM	LGM	LGM		

https://doi.org/10.5194/cp-2020-147
Preprint. Discussion started: 21 November 2020

Climate of the Past Discussions
Open Access
EGU

Table 2. Variables passed between GCM/WRF and LPJ-LMfire.

GCM/WRF to LPJ-LMfire	
30-year monthly values	
mean temperature at 2 m	convective available potential energy
daily max. temperature at 2 m	horizontal wind velocity at 10 m
daily min. temperature at 2 m	precipitation (liquid and solid)
total cloud cover fraction	

LPJ-LMfire to WRF	
30-year monthly values	climatological value
green vegetation cover (fraction)	land cover fraction (category)
leaf area index	dominant land cover type (category)
	soil temperature

https://doi.org/10.5194/cp-2020-147
Preprint. Discussion started: 21 November 2020

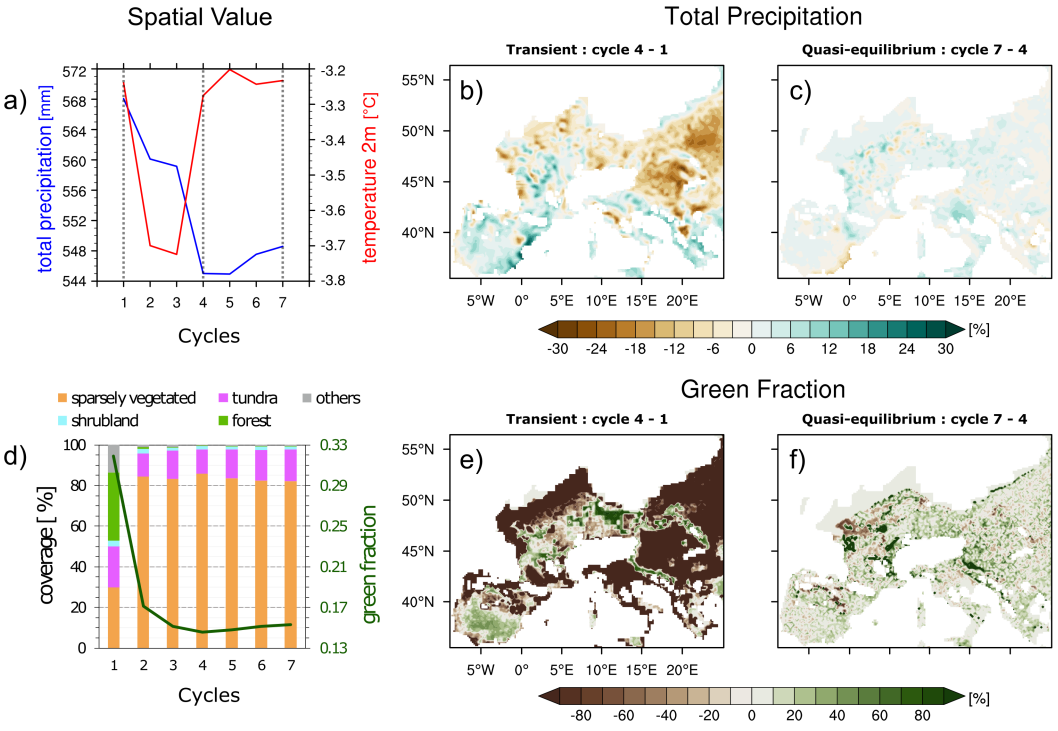

Figure 2. 30-year climatology of annual mean values throughout the iterations. Panel (a) represents the spatial mean values for total precipitation (blue line) and temperature at 2 m (red line), (b) the precipitation difference between the first and fourth iteration (transient). Panel (c) as (b) but fourth and seventh iteration (quasi-equilibrium). Panel (d) represents the percentage spatial fraction of bare (orange), tundra (pink), shrubland (sky blue), forest (light green), others (gray), and the spatial mean value of green vegetation fraction (dark green line). Panels (e) and (f) as (b) and (c) but for green fraction (i.e. green vegetation cover). The grey dotted lines in (a) represent the first, fourth and seventh iterations

https://doi.org/10.5194/cp-2020-147
Preprint. Discussion started: 21 November 2020

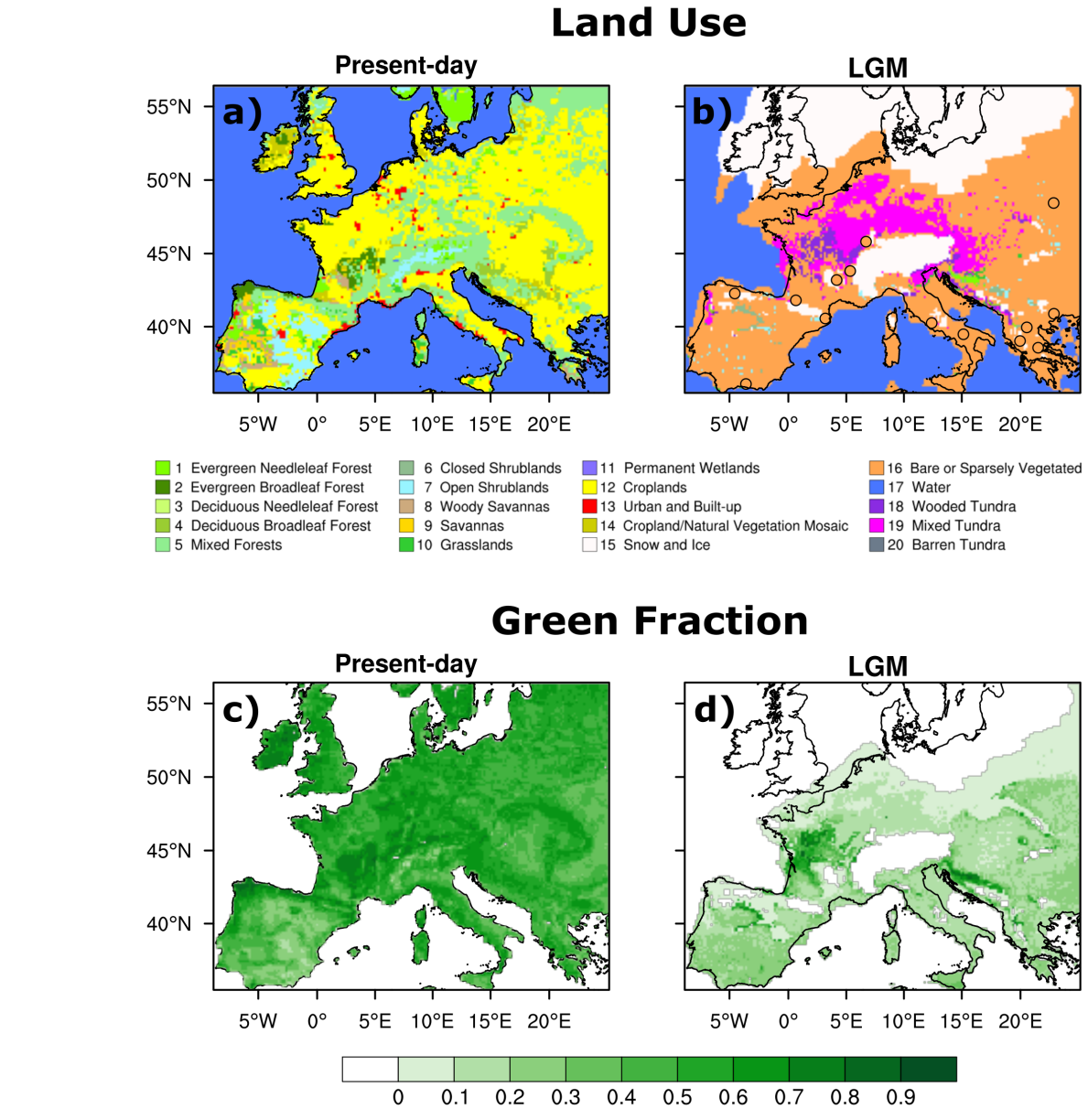

Figure 3. Land cover used by WRF. Panel (a) represents the land use (i.e., dominant land cover category) during present day. Panel (b) as (a) but during the LGM. Panels (c) and (d) as (a) and (b) but for green fraction (i.e., green vegetation cover).

https://doi.org/10.5194/cp-2020-147
Preprint. Discussion started: 21 November 2020

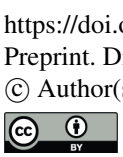

Climate of the Past
Discussions
Open Access
EGU

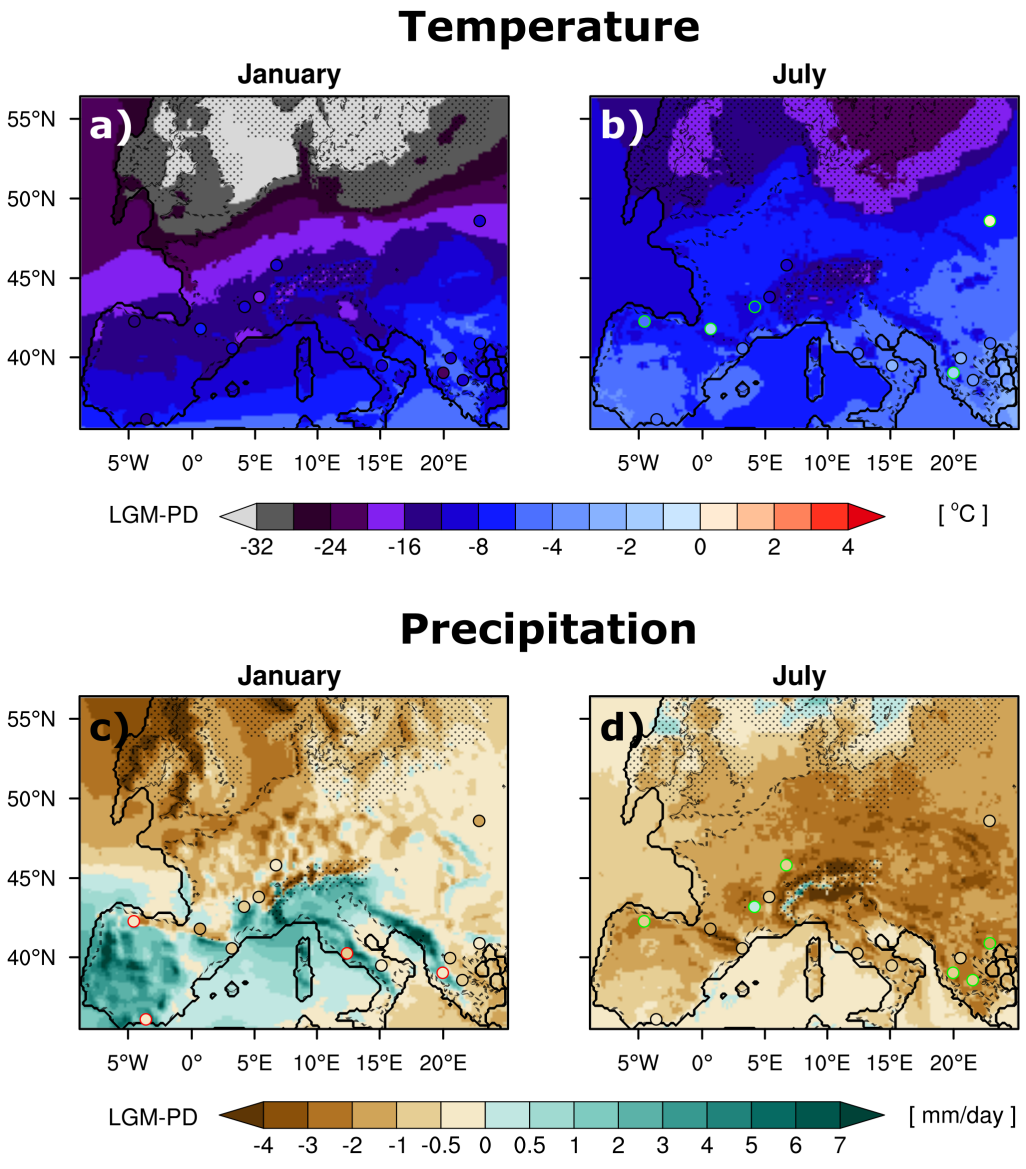

Figure 4. Changes in temperature and precipitation. Panel (a) represents the temperature differences between LGM and PD ($LGM_{LGM} - PD_{PD}$) for January. Panel (b) as (a) but for July. Panels (c) and (d) as (a) and (b) but for precipitation differences. Circles represent proxy evidences: a red (green) border indicates that the simulated value is significantly above (below) the proxy value at the closest grid cell of the model (outside the 90 % confidence interval, Wu et al., 2007). Solid line represents the LGM coastline, dashed line present-day coastline and dots the area covered by glaciers.

https://doi.org/10.5194/cp-2020-147
Preprint. Discussion started: 21 November 2020

Climate of the Past Discussions
Open Access
EGU

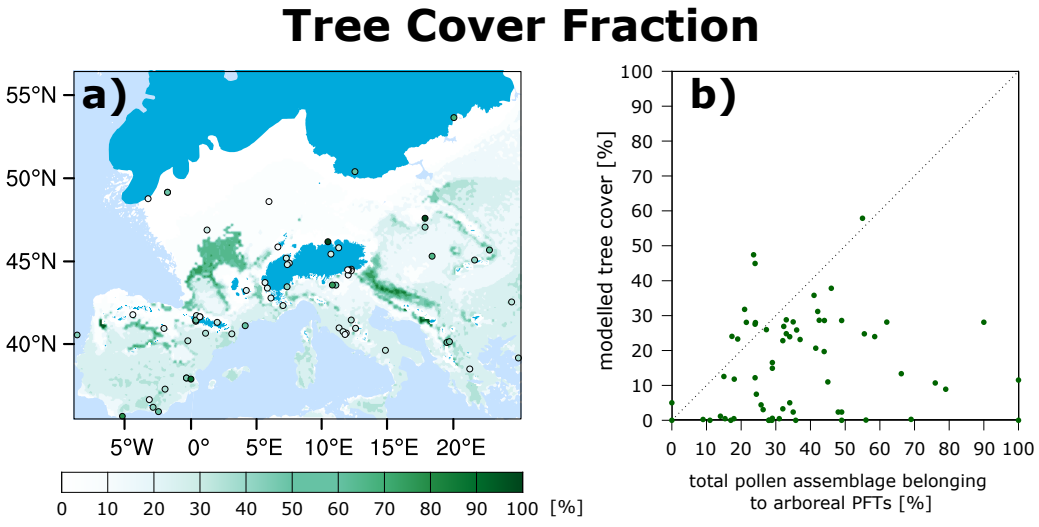

Figure 5. Comparison between modelled and reconstructed tree cover. Panel (a) represents the LPJ-LMfire simulated tree cover fraction from LGM_{LGM}. Circles represent the 71 pollen samples securely dated to LGM from Kaplan et al. (2016). Panel (b) shows a scatterplot of reconstructed vs. modelled LGM tree cover.

https://doi.org/10.5194/cp-2020-147
Preprint. Discussion started: 21 November 2020

Climate of the Past Discussions

Table 3. Assessment of the atmospheric response using precipitation and temperature. First column indicates the simulations that are compared, second column the annual response, and the other columns the response in each season. Note that the assessment considers land areas without snow/ice that are shared by both LGM and PD climate and discards the continental shelves exposed at the LGM.

	Annual	**DJF**	**MAM**	**JJA**	**SON**
Temperature response [°C]					
LGM_{LGM} - PD_{PD}	-11.99	-15.34	-13.85	-7.24	-11.53
LGM_{LGM} - LGM_{PD}	0.07	0.10	-0.66	0.85	-0.01
LGM_{PD} - PD_{PD}	-12.06	-15.44	-13.19	-8.09	-11.52
Precipitation response [mm day^{-1}]					
LGM_{LGM} - PD_{PD}	-0.67	0.09	-0.86	-1.55	-0.37
LGM_{LGM} - LGM_{PD}	-0.14	-0.07	-0.09	-0.40	0
LGM_{PD} - PD_{PD}	-0.53	0.16	-0.77	-1.15	-0.37

https://doi.org/10.5194/cp-2020-147
Preprint. Discussion started: 21 November 2020

Climate of the Past
Discussions
Open Access
EGU

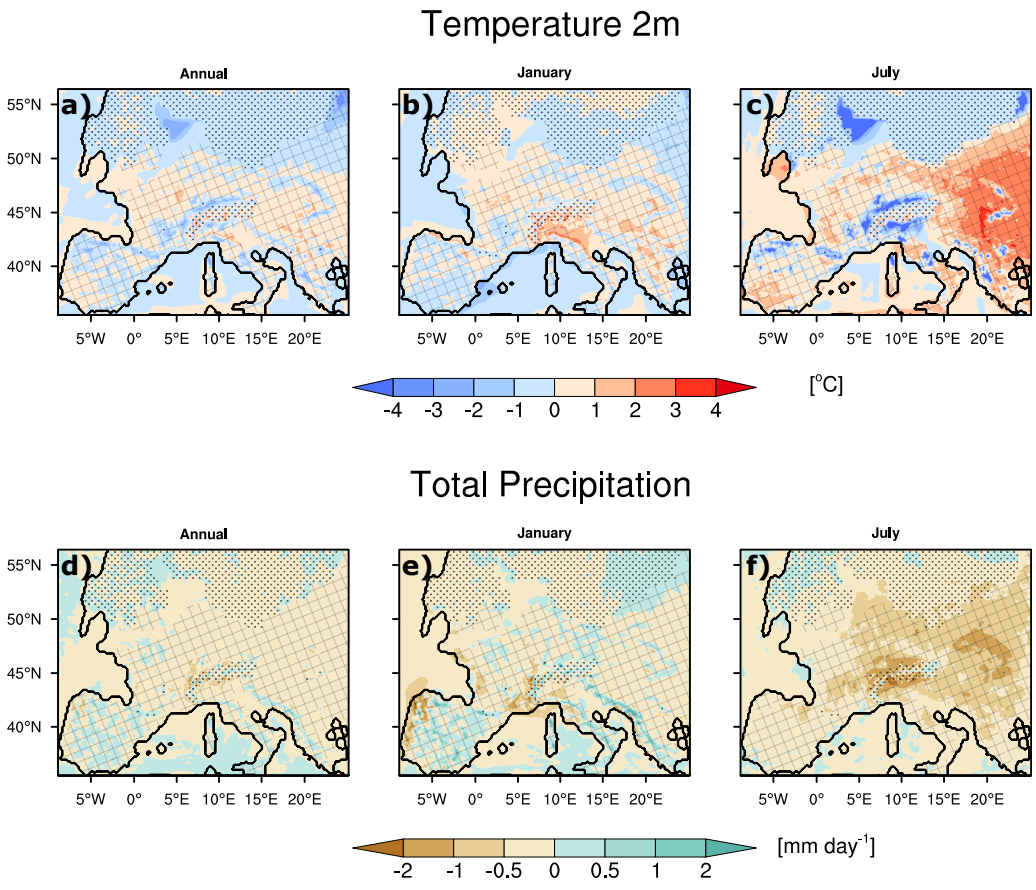

Figure 6. Atmospheric response to changes in the land cover. Panel (a) represents differences in the annual mean temperature between $\mathrm{LGM_{LGM}}$ – $\mathrm{LGM_{PD}}$. Panels (b) and (c) as (a) but for January and July, respectively. Panels (d), (e) and (f) as (a), (b) and (c) but for precipitation. The solid line represents the coastline during the LGM, stippled areas are covered by glaciers and crosshatched areas are considered in the spatial climatology.